

Exploring triple Higgs production at the LHC and beyond to constrain trilinear and quartic Higgs couplings

Panagiotis Stylianou^a and Georg Weiglein^{a,b,*}

^aDeutsches Elektronen-Synchrotron DESY, Notkestr. 85, 22607 Hamburg, Germany

^bInstitut für Theoretische Physik, Universität Hamburg, Luruper Chaussee 149, 22761 Hamburg, Germany

E-mail: panagiotis.stylianou@desy.de, georg.weiglein@desy.de

The understanding of the shape of the Higgs potential requires experimental information on the Higgs boson self-couplings. While current experiments already provide some insights on the trilinear self-coupling κ_3 through Higgs pair production, important information will also become accessible from the production process of three Higgs bosons in the future runs of the LHC. Even though this process suffers from small cross sections, it is of particular interest since it depends on both κ_3 and the quartic self-coupling κ_4 . Using Graph Neural Networks we investigate the feasibility of constraining the Higgs self-couplings through HHH production and find that the HL-LHC can be sensitive to large deviations from the SM that are allowed by the constraints from tree-level perturbative unitarity and in an effective field theory treatment are compatible with the present bounds on κ_3 . We additionally address the prospects of lepton colliders operating at the TeV energy range.

*The European Physical Society Conference on High Energy Physics (EPS-HEP2023)
21-25 August 2023
Hamburg, Germany*

*Speaker

1. Introduction

The discovery of a Higgs boson at the LHC has enacted a tremendous effort for measuring its couplings and understanding its properties. Of particular importance are the Higgs self-couplings which provide information about the shape of the Higgs potential. While in the SM the Higgs potential is given by

$$V(\Phi) = \lambda(\Phi^\dagger\Phi)^2 - \mu^2\Phi^\dagger\Phi \quad (1)$$

and is characterised by λ and μ , or equivalently the Higgs mass M_H and vacuum expectation value (VEV) v , models with extended scalar sectors could have richer and more complicated structures. Gaining information about the actual shape without assuming from the start a particular form of the potential (as the one of the SM) is thus dependent on the ability to measure the trilinear and quartic Higgs self-couplings. Experimental constraints can be expressed in terms of the κ -framework, where deviations from the SM lowest order couplings are defined as $\kappa_i = g_i/g_i^{\text{SM}}$ for $i = 3, 4$ denoting the trilinear and quartic coupling, respectively.

Current experiments can constrain κ_3 through Higgs pair production combining gluon-fusion and Weak Boson Fusion (WBF) production channels [1, 2]. ATLAS [1] provides the currently most stringent 95% C.L. bound of $\kappa_3 \in [-0.4, 6.3]$ by combining different HH production channels with data from single Higgs boson production. Triple Higgs production, while known to suffer from small cross sections, could provide additional information on κ_3 and the first experimental constraints on κ_4 .

In this work, we motivate that large deviations on κ_4 are possible and discuss the bounds from perturbative unitarity in Sec. 2 together with the correlation between κ_3 and κ_4 in an effective field theory treatment. We explore the potential constraints at HL-LHC from the $6b$ and $4b2\tau$ final states in Sec. 3 and also discuss bounds from lepton colliders in Sec. 4. We conclude in Sec. 5.

2. Current bounds, unitarity and theoretical motivation

Theoretical bounds from perturbative unitarity can be placed on the self-couplings by decomposing the $HH \rightarrow HH$ scattering amplitude to partial waves. We calculate the tree-level zeroth partial wave a^0 for different values of κ_3 and κ_4 at various energies (similarly to Ref. [3]) and show the obtained bounds from requiring $|\text{Re}(a_{ii}^0)| \leq 1/2$ in Fig. 1. We additionally show the current experimental constraints on the trilinear coupling and the HL-LHC 95% C.L. combined ATLAS and CMS projection, $\kappa_3 \in [0.1, 2.3]$ [4]. The theoretical constraints on κ_3 are considerably stronger than on κ_4 , which can be understood in terms of an effective field theory (EFT) prescription.

Considering a generic extension of the SM potential in inverse powers of a UV-scale Λ using powers of $(\Phi^\dagger\Phi - v^2/2)$ (see Refs. [5, 6]), where Φ is the SM doublet and v the Higgs VEV, one can write the coupling modifiers as

$$(\kappa_3 - 1) = \frac{C_6 v^2}{\lambda \Lambda^2}, \quad (\kappa_4 - 1) = \frac{6C_6 v^2}{\lambda \Lambda^2} + \frac{4C_8 v^4}{\lambda \Lambda^4}. \quad (2)$$

Here C_6 (C_8) denotes the coefficient of the dimension-six (-eight) operator in the power expansion. Requiring that the dimension-eight effects on κ_4 are smaller than the dimension-six ones yields $|(\kappa_4 - 1) - 6(\kappa_3 - 1)| < 6|\kappa_3 - 1|$ (shown as a shaded region in Fig. 1). This correlation between

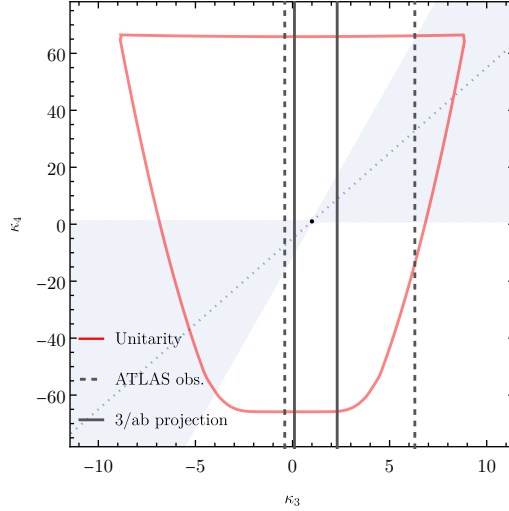


Figure 1: Bounds from perturbative unitarity along with current (projected) experimental constraints are shown as red and (dashed) black lines, respectively. The shaded light blue region denotes the region where dimension-eight effects on κ_4 are smaller than the ones of dimension-six if one extends the SM potential with higher-dimensional operators, while the dashed blue line indicates where the dimension-eight contribution exactly vanishes, $\kappa_4 - 1 \simeq 6(\kappa_3 - 1)$.

κ_3 and κ_4 shows that deviations on the quartic coupling can be more sizeable than the ones to the trilinear coupling, in-line with the weaker constraints of perturbative unitarity on κ_4 . Thus, if a certain correction is induced in κ_3 one would expect from the perspective of an EFT with high scale cutoff where the dimension-eight terms are negligible that the deviation in κ_4 from the SM value should be six times larger than the one in κ_3 . Similar results are also obtained for renormalisable models as for example the Two-Higgs Doublet Model (2HDM). Loop-level effects induced by mass splittings between the additional Higgs bosons of the 2HDM yield substantial shifts in κ_3 (see e.g. Ref. [7]), and it can be shown that the corresponding corrections entering κ_4 are significantly larger.

3. Triple Higgs production at the HL-LHC

To investigate the feasibility of constraining κ_3 and κ_4 through triple-Higgs production at the HL-LHC we focus on production through gluon fusion with decays of on-shell Higgs bosons to b -quarks and τ -leptons. We consider the $6b$ and $4b2\tau$ final states requiring that at least 5 and 3 b -jets are reconstructed and b -tagged. The dominant background for the $6b$ channel arises from multi-jet QCD events, while the $4b2\tau$ state receives contributions from $WWbbbb$ (including $ttbb$), $Zbbbb$, ttH ttZ and the four-top production. All signal and background events are generated with MADGRAPH [8, 9] with a minimum invariant mass of the process of 350 GeV. We impose $p_T(b) > 30$ GeV, $p_T(\tau) > 10$ GeV, $|\eta(b)| < 2.5$, $|\eta(\tau)| < 2.5$ and at least one pair of b -jets or τ -leptons close to the Higgs mass [110, 140] GeV. We assume a signal (background) K-factor of 1.7 [10] (2) with tagging efficiencies of 0.8. At least one τ is assumed to decay hadronically.

The signal for each channel is selected by a tuned Graph Neural Network (GNN) utilising the EdgeConv [11] operation, after training on the simulated signal data with $(\kappa_3, \kappa_4) = (1, 1)$ for both

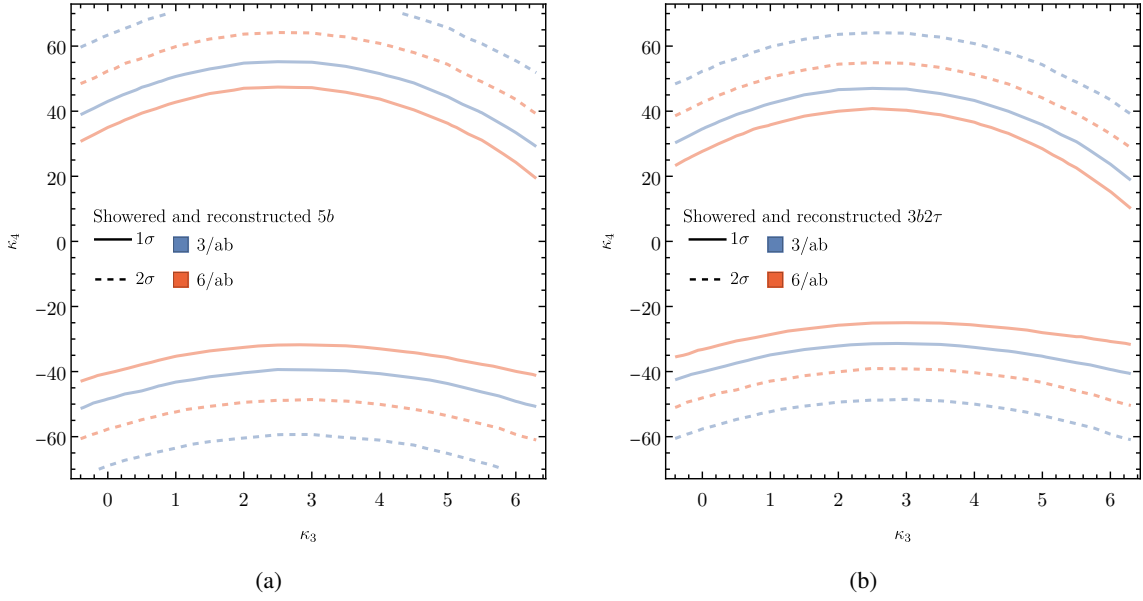


Figure 2: Contours in the κ_3 - κ_4 plane from two different final-states of triple Higgs production at the LHC.

channels.¹ For the $5b$ analysis the signal region is then selected by requiring a background rejection of $\sim 0.6\%$, while for the $3b2\tau$ analysis the following criteria must be satisfied by the GNN score: $P[WWbbbb] < 3\%$, $P[Zbbbb] < 10\%$ and $P[tt(H \rightarrow \tau\tau)] < 30\%$.

The significance Z for each channel is then calculated with the signal events S and background events B that remain in the selection region, using

$$Z = \sqrt{2 \left((S+B) \ln \left(1 + \frac{S}{B} \right) - S \right)}. \quad (3)$$

We assume a HL-LHC luminosity of $3/\text{ab}$ and also consider a combined ATLAS and CMS luminosity of $6/\text{ab}$, showing the resulting 1σ and 2σ bounds in Fig. 2.

4. Reach assessment for lepton colliders

We finally explore the possible bounds on κ_3 and κ_4 at different proposed lepton colliders through an inclusive $\ell\ell \rightarrow HHH + X$ analysis, capturing effects from the associated Z -Higgs and Weak Boson Fusion (WBF) channels.² Here we only focus on the decay of the Higgs bosons to $b\bar{b}$, requiring at least five b -jets.

As in the LHC case, we require the p_T of b -quarks to exceed 30 GeV and assume a b -tagging efficiency of 0.8. When considering low-energy collisions at around ~ 1 TeV, the b quarks are produced in the central part of the detector, $|\eta(b)| < 2.5$. However, at high energies b quarks can be produced with a wider range of pseudo-rapidities. It is thus beneficial to consider detectors with extended capabilities in tagging and allow $|\eta(b)| < 4$.

¹For the $4b2\tau$ analysis, we train the network for multi-class classification only on $WWbbbb$, $Zbbbb$ and $tt(H \rightarrow \tau\tau)$ background contributions which we find sufficient to reject other background sources as well.

²These channels have been separately studied in Refs. [6, 12] for certain concepts.

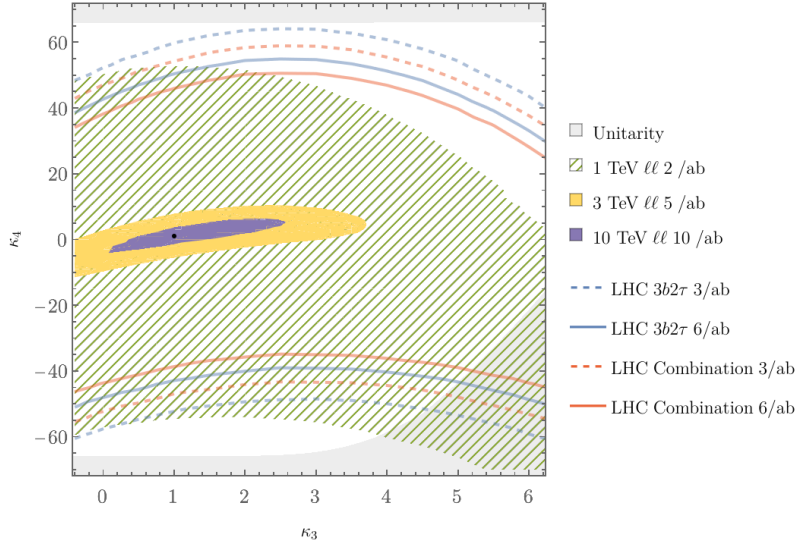


Figure 3: 95% enclosed regions are shown for lepton colliders with 1, 3 and 10 TeV at different integrated luminosities. The blue lines show the $4b2\tau$ results at HL-LHC for comparison and the red line shows a combination of $6b$ and $4b2\tau$ at the LHC assuming no correlations. The region that is excluded by the unitarity constraint is shown as a shaded gray area.

Lepton colliders provide a clean environment avoiding large QCD backgrounds. For a signal region enforcing a total invariant mass for the process of at least 350 GeV and one b -pair close to the Higgs mass, no background events are expected. A Poissonian analysis is then applicable, with the upper limit on the mean value μ of the Poisson distribution given by

$$\mu_{\text{up}} = \frac{1}{2} F_{\chi^2}^{-1} \left[2(n+1); \text{CL} \right], \quad (4)$$

where n denotes the expected events for the SM. F_{χ^2} is the cumulative distribution function of the χ^2 distribution, and CL indicates the confidence level. We show the resulting limits in Fig. 3 for different collision energies at different assumed integrated luminosities.

5. Conclusions

Our study indicates that even though triple-Higgs production is limited by low rates at the LHC, its exploration provides interesting information even if it does not receive additional contributions from extra scalar resonances. Bounds can be placed on κ_4 beyond the theoretical constraints from perturbative unitarity. While as expected the bounds on κ_3 will be much weaker than the ones from double-Higgs production, they should be useful for improving the sensitivity through combinations. Additionally, if deviations are found, the correlation between the Higgs self-couplings can shed light on the possible scenarios of physics beyond the SM. The HL-LHC results for κ_4 should be competitive with a 1 TeV lepton collider such as ILC. The limits from lepton collisions at 3 and 10 TeV (e.g. CLIC or a possible muon-collider) are considerably stronger, but they will presumably become available only on a longer time scale, such as the ones from a future higher-energetic hadron

collider. Thus, it can be expected that the HL-LHC will be able to establish the first bounds on κ_4 beyond theoretical considerations.

Acknowledgements — This work is supported by the Deutsche Forschungsgemeinschaft under Germany’s Excellence Strategy EXC2121 “Quantum Universe” - 390833306 and has been partially funded by the Deutsche Forschungsgemeinschaft (DFG, German Research Foundation) - 491245950.

References

- [1] ATLAS collaboration, G. Aad et al., *Constraints on the Higgs boson self-coupling from single- and double-Higgs production with the ATLAS detector using pp collisions at $s=13$ TeV*, *Phys. Lett. B* **843** (2023) 137745, [[2211.01216](#)].
- [2] CMS collaboration, A. Tumasyan et al., *A portrait of the Higgs boson by the CMS experiment ten years after the discovery*, *Nature* **607** (2022) 60–68, [[2207.00043](#)].
- [3] T. Liu, K.-F. Lyu, J. Ren and H. X. Zhu, *Probing the quartic Higgs boson self-interaction*, *Phys. Rev. D* **98** (2018) 093004, [[1803.04359](#)].
- [4] M. Cepeda et al., *Report from Working Group 2: Higgs Physics at the HL-LHC and HE-LHC*, *CERN Yellow Rep. Monogr.* **7** (2019) 221–584, [[1902.00134](#)].
- [5] F. Boudjema and E. Chopin, *Double Higgs production at the linear colliders and the probing of the Higgs selfcoupling*, *Z. Phys. C* **73** (1996) 85–110, [[hep-ph/9507396](#)].
- [6] F. Maltoni, D. Pagani and X. Zhao, *Constraining the Higgs self-couplings at e^+e^- colliders*, *JHEP* **07** (2018) 087, [[1802.07616](#)].
- [7] H. Bahl, J. Braathen and G. Weiglein, *New Constraints on Extended Higgs Sectors from the Trilinear Higgs Coupling*, *Phys. Rev. Lett.* **129** (2022) 231802, [[2202.03453](#)].
- [8] J. Alwall, R. Frederix, S. Frixione, V. Hirschi, F. Maltoni, O. Mattelaer et al., *The automated computation of tree-level and next-to-leading order differential cross sections, and their matching to parton shower simulations*, *JHEP* **07** (2014) 079, [[1405.0301](#)].
- [9] V. Hirschi and O. Mattelaer, *Automated event generation for loop-induced processes*, *JHEP* **10** (2015) 146, [[1507.00020](#)].
- [10] D. de Florian, I. Fabre and J. Mazzitelli, *Triple Higgs production at hadron colliders at NNLO in QCD*, *JHEP* **03** (2020) 155, [[1912.02760](#)].
- [11] Y. Wang, Y. Sun, Z. Liu, S. E. Sarma, M. M. Bronstein and J. M. Solomon, *Dynamic Graph CNN for Learning on Point Clouds*, *arXiv e-prints* (Jan., 2018) [arXiv:1801.07829](#), [[1801.07829](#)].
- [12] M. Gonzalez-Lopez, M. J. Herrero and P. Martinez-Suarez, *Testing anomalous $H - W$ couplings and Higgs self-couplings via double and triple Higgs production at e^+e^- colliders*, *Eur. Phys. J. C* **81** (2021) 260, [[2011.13915](#)].